Journal of Materials Chemistry A

Accepted Manuscript

ROYAL SOCIETY OF CHEMISTRY

www.rsc.org/materialsA

Journal of Materials Chemistry A

PAPER

Pseudopolymorphic seeding for rational synthesis of hybrid membranes with zeolitic imidazolate framework for enhanced molecular separation performance

Received 00th January 20xx,
Accepted 00th January 20xx

DOI: 10.1039/x0xx00000x

www.rsc.org/

Yang Lo[a] and Dun-Yen Kang*[a]

This paper reports a novel methodology involving the use of pseudopolymorphic seeding for the rational synthesis of hydrogen-selective hybrid membranes with zeolitic imidazolate frameworks (ZIFs). A proof-of-concept was demonstrated using two-dimensional layered ZIF-L as seed crystals for the growth of its pseudopolymorph ZIF-8 in the formation of ZIF-L@ZIF-8 hybrid membranes. This approach enables the incorporation of ZIF-L (with high hydrogen diffusivity) within the ZIF-8 matrix with a volume fraction of ZIF-L of approximately 28%. Compared with conventional secondary growth methods used in the synthesis of pure ZIF-8 membranes, we employed leaf-like ZIF-L with a high aspect ratio as seed crystals for the growth of ZIF-8 membranes with a preferred orientation along the <100> direction. Compared to pure ZIF-8 membranes, the ZIF-L@ZIF-8 hybrid membranes enable a three-fold enhancement in hydrogen permeability and increase the permeative selectivity of hydrogen-over-carbon dioxide from 2.3 to 4.7. Simulation of mass transfer at the microscopic level was used to elucidate the reasons for the enhanced performance of the membrane in gas separation. We determined that the interlayer spacing among ZIF-L crystals, which allows for the rapid diffusion of hydrogen, is probably the key reason for the high separation performance of the ZIF-L@ZIF-8 hybrid membranes.

Introduction

Thermally-driven molecular separation processes (e.g., absorption, adsorption, and distillation) are highly energy-intensive. Pressure driven membrane-based processes have been developed as a low-energy alternative with limited environmental impact.[1-3] Polymeric membranes are the dominant materials used in membrane separation, due to their low cost and suitability for large-scale fabrication. Nonetheless, there remain a number of challenges in the fabrication of polymeric membranes, including issues related to thermal and chemical stability as well as the trade-off between selectivity and permeability.[3-6] Efforts to address these limitations led to the development of crystalline microporous materials, such as zeolites and metal-organic frameworks (MOFs) as alternative materials for membrane-based molecular separation. For over two decades, researchers have been developing zeolite membranes for gas separation. Several of these separation systems, such as o-xylene-and-p-xylene mixtures, present excellent separation performance;[7] however, the broader application of zeolite membranes has been limited by the number of available synthetic zeolites.[8, 9] MOF materials synthesized from metal salts and organic ligands provide diversity greater than that of zeolites, due to the fact that new MOFs can be easily synthesized whenever new ligands become available.

Zeolitic imidazolate frameworks (ZIFs) are an emerging subset of MOFs comprising an imidazolate building unit within a zeolite-type topology.[10-13] Due to their high surface area and excellent thermal and chemical stability,[14] ZIFs have been widely applied for the capture and storage of CO_2[15, 16] as well as in catalysts,[17] sensors,[18] and biomedical applications.[19] Their precisely defined pore size and interior surface functionality have attracted considerable interest among researchers for the preparation of ZIF membranes for molecular separations.[10, 20, 21]

The fabrication of defect-free ZIF membranes is far more challenging than the relatively straightforward synthesis of ZIF crystals. Over the past five years, several approaches have been developed for the synthesis of pure ZIF membranes on a substrate for the process of separation. The *in situ* growth of ZIF membranes can be achieved by immersing a substrate in a precursor solution to permit the simultaneous occurrence of nucleation and crystal growth on the substrate.[22] However, without an efficient mechanism for the heterogeneous nucleation of ZIF crystals on the substrate, the formation of high-quality membranes becomes problematic. Secondary growth methods are the most common approach to the synthesis of ZIF membranes. This method involves two steps: the seeding of crystals on a substrate followed by the growth of membrane on the surface of the seed crystals. A dense uniform seed layer is usually sufficient to guarantee the successful growth of membranes.[23-26] Improvements in the secondary growth process have been achieved by introducing various surface modifications with the aim of enhancing interfacial affinity between the

[a] *Department of Chemical Engineering, National Taiwan University, Taipei, Taiwan.*
**E-mail: dunyen@ntu.edu.tw*

†Electronic Supplementary Information (ESI) available: SEM images, FT-IR spectra, XRD patterns and illustration of proprietary membrane permeation setup. See DOI: 10.1039/x0xx00000x

substrate and seed crystals.[27-31] Reactive seeding was proposed for heterogeneous surface reactions used in the formation of seed crystals on a substrate.[32] Advancements in seeding have allowed for the growth of highly-oriented MOF crystals with the membranes.[33] Secondary growth processes using seed crystals that differ from the materials used in the growth of the membrane have also been reported.[34, 35] Advances in fabrication of ZIF membranes include the interfacial counter diffusion of metal ions and the dissolving of ligands for deposition as a ZIF layer on the substrate.[36, 37] This approach has been extended to a directing of ZIF membranes on hollow fiber support.[38] Recently, ZIF membrane synthesis with chemical modification and chemical modification assisted methods have been reported.[24, 28, 39, 40] Efforts in the fabrication of ZIF membranes have been focused on improving process efficiency or minimizing defects in membranes. However, the creation of new ZIF membranes with high separation performance requires rational engineering.

This paper introduces a novel approach involving pseudopolymorphic seeds to the synthesis of hybrid ZIF membranes with enhanced separation performance. A proof-of-concept was demonstrated using ZIF-L as a seed crystal in the secondary growth of its pseudopolymorph ZIF-8 in the fabrication of ZIF-L@ZIF-8 hybrid membranes (Fig. 1a). ZIF-L was first synthesized in 2013.[41] It possesses a two-dimensional layered structure and forms as leaf-like crystals (Fig. 1b and 1c).[41-44] The objective behind the use of pseudopolymorphic seeding based on ZIF-L is three-fold. First, the high aspect ratio of ZIF-L crystals could be used to control crystal orientation in the subsequent growth of ZIF-8 (Fig. 1d and 1e). Second, the pseudopolymorphs of ZIF-L and ZIF-8 provide excellent interfacial affinity during the secondary growth of ZIF-8 on ZIF-L, as demonstrated in our previous work.[43] Third, interlayer spacing within ZIF-L crystals enables the rapid diffusion of molecules; therefore, incorporating ZIF-L within hybrid membranes could help to enhance separation performance. ZIF-L@ZIF-8 membranes were fabricated on macroporous alumina substrates through aqueous synthesis. The morphology and microstructure of the resulting membranes were carefully characterized using scanning electron microscopy (SEM), X-ray diffraction (XRD), and FT-IR spectroscopy. Single gas permeation with hydrogen, methane, nitrogen, and carbon dioxide was used to evaluate the separation performance of the membranes. Finally, we performed simulations of mass transfer at the microscopic level to gain insight into the diffusion of gas through the hybrid membranes.

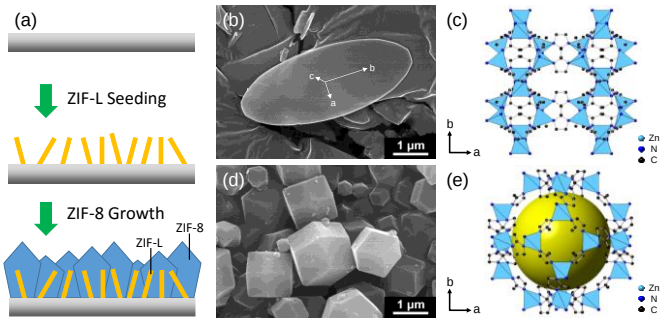

Fig. 1. (a) Schematic illustration of ZIF-L@ZIF-8 membrane synthesis (b) SEM image and (c) structure of ZIF-L crystal; (d) SEM image and (e) structure of ZIF-8 crystal

Experimental section

Chemicals

Zinc nitrate hexahydrate (Zn(NO3)2·6H2O, >98%), 2-Methylimidazole (C4H6N2, >99%) and sodium formate (NaCOOH, >99%) were purchased from Sigma-Aldrich. All chemicals were used without further purification. The deionized water used for the synthesis was purified using the Thermo Scientific™ Barnstead™ NANOpure® DIamond™ analytical ultrapure water system.

Synthesis of ZIF-L and ZIF-8 Seed Layers

The precursor solution for the synthesis of the ZIF-L seed layer was prepared using a method outlined in a previous report[41] with minor modifications. Briefly, 0.66 g of 2-methylimidazole and 0.14 g of sodium formate were dissolved in 20 mL of deionized water. A separate solution formed by dissolving 0.30 g of zinc nitrate hexahydrate in 20 mL of deionized water was added to the previous mixture to form the synthesis solution. This synthesis solution was transferred to a Teflon® liner with a capacity of 50 mL. An α-Alumina substrate was cleaned by sonicating in deionized water and dried in a convection oven at 100 °C before being placed vertically in the Teflon® liner with the synthesis solution. The mixture was stirred at room temperature under 1 atmosphere for 2 hours to form the ZIF-L seed layer on the substrate. The substrate was then gently rinsed with deionized water using a plastic pipette and dried at room temperature. The α-Alumina substrate with ZIF-L seed layer was used in the subsequent growth of the membrane.

The precursor solution used to produce the ZIF-8 seed layer was prepared in accordance with the methods outlined in a previous[26] study with minor modifications. Briefly, 2.27 g of 2-methylimidazole and 0.11 g of zinc nitrate hexahydrate were dissolved in 40 mL of deionized water. This mixture was transferred to a Teflon® liner with a capacity of 50 mL. An α-Alumina substrate was cleaned using the method mentioned above and placed vertically in the Teflon® liner with the synthesis solution. The mixture was stirred at room temperature under 1 atmosphere for 2 hours to form the ZIF-8 seed layer on the substrate. The substrate was then gently rinsed with methanol using a plastic pipette and dried at room temperature. The α-Alumina substrate with ZIF-8 seed layer was used in the subsequent growth of the membrane.

Growth of Hybrid ZIF-L@ZIF-8 and Pure ZIF-8 Membranes

The solution used for the second growth of ZIF-8 crystals was prepared in accordance with the methods outlined in a previous study.[26] To synthesis the ZIF-L@ZIF-8 hybrid membrane, a solution of 0.11 g of zinc nitrate hexahydrate and 2.27 g of 2-methylimidazole was dissolved in 40 mL of deionized water in a Teflon® jar with a capacity of 50 mL. The α-Alumina substrate with ZIF-L seed layer was placed vertically in the Teflon® jar.

The synthesis solution was stirred at room temperature under 1 atmosphere for 6 hours during the growth of the ZIF-8 layer on the ZIF-L seed layer. Following synthesis, the substrate was rinsed gently with methanol using a plastic pipette. The substrate was then immersed in methanol for 24 hours and dried at room temperature. The resulting substrate with ZIF-L@ZIF-8 hybrid membrane was used for characterization. The synthesis of pure ZIF-8 membranes followed the same methods as those for the ZIF-L@ZIF-8 hybrid membranes, except that the α-Alumina substrate was coated with a seed layer of ZIF-8, instead of ZIF-L.

Characterization

The morphology of all solid-state samples was characterized using a Hitachi S-4800 Field Emission scanning electron microscope (SEM) with Energy Dispersive Spectrometer (EDS) operated at an accelerated voltage of 20 kV. Grazing-incidence X-ray diffraction (GIXRD) was performed on thin film samples using a PAnalytical X'pert diffractometer operated with a Cu Kα source, scanning from 5 to 30° 2θ with a step size of 0.02°. FT-IR spectra of the thin film samples were recorded in attenuated total reflection (ATR) mode using a JASCO FT/IR-6700 spectrometer with Ge coated KBr beam splitter. The ATR accessory was equipped with a diamond crystal. Each FT-IR spectrum is the compilation of 100 scans at a resolution of 4 cm^{-1}. Single gas permeation for the prepared membrane samples was performed using a proprietary setup (ESI,† Fig. S1). Prior to measurement, a membrane sample was placed within a sealed cell and degassed under 0.05 torr at room temperature for at least 24 hours. During measurement, the upstream of the cell was exposed to the target gas (H_2, N_2, CH_4, or CO_2) at a pressure of 2 bar with the downstream of the cell exposed to the atmosphere. A bubble flow meter was used to measure the volumetric flow rate of the target gas downstream. The volumetric flow rate of gas was then converted to derive the permeability of the membrane for this gas.

Simulation of Mass Transfer

The simulation of mass transfer in the heterogeneous ZIF-L@ZIF-8 hybrid membranes was conducted according to the methodology described in our previous work.[45-47] Briefly, a model was constructed with layered objects in a box in order to model the layered ZIF-L crystals in the membrane. The volume fraction of the layered objects in box was set to be 28% for mimicking the experimentally measured volume fraction of ZIF-L. We assumed that mass transfer in the hybrid membrane is governed by Fick's law of diffusion:

$$\vec{J}=-D\cdot\vec{\nabla}C \quad (1)$$

where $\vec{J}$ is the flux vector of the transported species, D is diffusivity, and $\vec{\nabla}C$ is the concentration gradient vector of the transported species. The diffusivity values of ZIF-8 was obtained for the simulations from measurements of single gas permeation using pure ZIF-8 membranes. The solubility of ZIF-8 and ZIF-L used to determine the interfacial concentration ratio at the ZIF-8-ZIF-L interfaces was found in the literature.[41, 48] The diffusivity of ZIF-L was adjusted until the permeability values in the simulations were in agreement with those obtained in experiments. Fick's equation of diffusion was numerically solved using finite element method in the commercialized package COMSOL Multiphysics®. This yielded the concentration profile of the system, which was then converted into the simulated values of permeability of the membranes.

Results and discussion

Morphology and Microstructure of Membranes

The morphology of the pure ZIF-8 and ZIF-L@ZIF-8 hybrid membranes was assessed using scanning electron microscopy (SEM). SEM images of the seed layers and membranes are presented in Fig. 2. Pure ZIF-8 membranes were prepared via secondary growth over a ZIF-8 seed layer. ZIF-L@ZIF-8 hybrid membranes were synthesized using the same method with ZIF-L as the seed crystals. Top and side views of the ZIF-L seed layers are presented in Fig. 2a and 2b. The ZIF-L seed crystals present a characteristic leaf-like morphology. They were uniformly distributed on the α-alumina substrate with a high degree of surface coverage. As reported in previous studies,[49, 50] uniformity and surface coverage both play a critical role in the subsequent process of secondary growth. It is worth noting that most of the ZIF-L crystals did not "lay down" completely on the substrate. This allowed the (001) facet of the ZIF-L crystals, which possesses a far larger surface area than the (100) and (010) facets, to direct the subsequent secondary crystal growth in the in-plane direction, i.e., the direction parallel to the surface of the substrate. The morphology of the ZIF-8 seed layers is presented in Fig. 2c and 2d, showing the high degree of surface coverage of the ZIF-8 crystals as well as uniform distribution on the substrate. The size of the ZIF-L crystals (4μm) is distinct from that of the ZIF-8 crystals (below 800 nm). A difference of this magnitude is likely to affect the thickness of the resulting membrane. SEM images of ZIF-L@ZIF-8 hybrid membranes, which were synthesized by growing ZIF-8 on ZIF-L seed crystals, are presented in Fig. 2e-2h. The ZIF-L@ZIF-8 hybrid membranes are dense and homogeneous with a total absence of defects and cracks at the micrometer scale. The leaf-like crystals in Fig. 5g suggest the ZIF-L crystals may have been preserved even after the secondary growth of ZIF-8 and provides a good indication that the synthesis of the hybrid membranes was successful. Good surface interaction between ZIF-L and ZIF-8 crystals in the hybrid membrane may be due to the fact that these two crystals are pseudopolymorphs. In our previous work, we reported that ZIF-8 has excellent surface affinity to ZIF-L.[43] Two-dimensional electron dispersive spectroscopy (EDS) was applied to cross-sectional SEM images of the hybrid membrane for elemental mapping (Fig. 2h), the results of which clearly reveal an interface between the membrane and alumina substrate. This provides additional supporting evidence of a dense ZIF membrane on the substrate. Additional SEM images of the ZIF-L seed layer and ZIF-L@ZIF-8 hybrid membranes are presented in ESI,† Fig. S2. According to the mass of the ZIF-L seed layer and that of ZIF-L@ZIF-8 hybrid membranes, the mass fraction of ZIF-L in the hybrid is about 36%, which is equivalent a ZIF-L volume

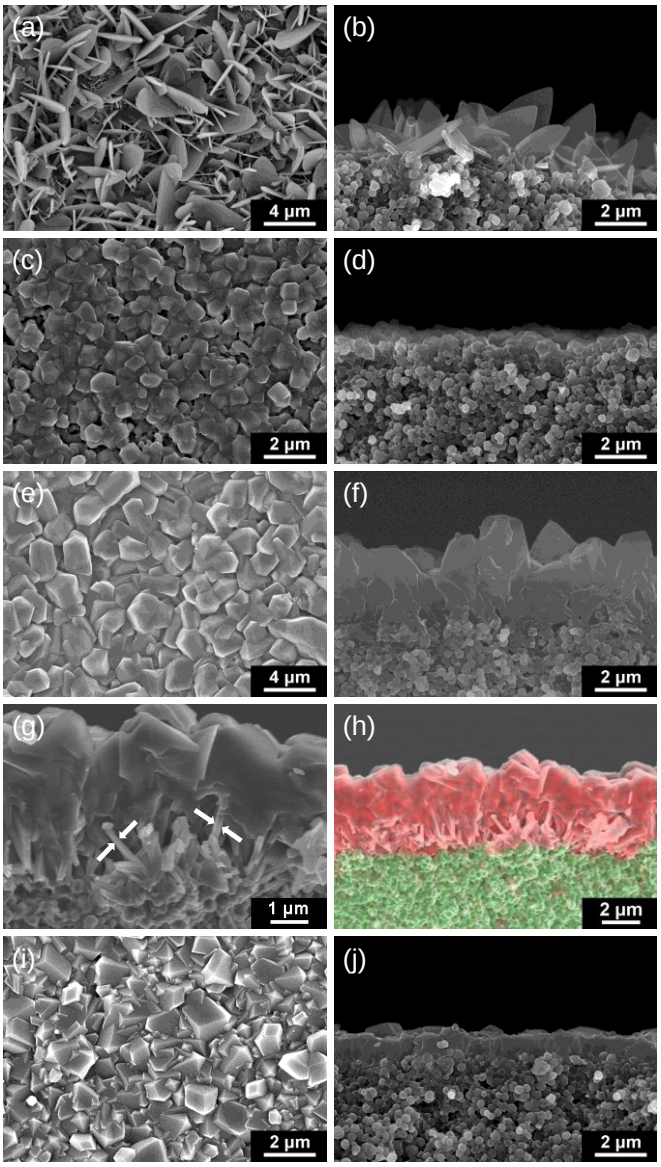

Fig 2. (a) Top-view and (b) side-view SEM images of ZIF-L seed layer; (c) top-view and (d) side-view SEM images of ZIF-8 seed layer; (e) top-view and (f) and (g) side-view SEM images of ZIF-L@ZIF-8 hybrid membrane; (h) SEM-EDS elemental mapping (Zn is in red and Al is in green); (i) top-view and (j) side-view SEM images of pure ZIF-8 membrane. The arrows in (g) indicate the location of ZIF-L nanoflake in the ZIF-L@ZIF-8 hybrid membrane.

fraction of approximately 28%. SEM images of pure ZIF-8 membranes synthesized via epitaxial secondary growth on ZIF-8 seed crystals are presented in Fig. 2i and 2j. As shown in top-surface images (Fig. 2e and 2f), the crystal grains in ZIF-L@ZIF-8 hybrid and pure ZIF-8 membranes are of similar size (within a few of micrometers); however, the difference in thickness between these two types of membrane is pronounced. Specifically, the thickness of the ZIF-L@ZIF-8 hybrid membrane is approximately 3.5 μm, whereas the pure ZIF-8 membrane is approximately 1 μm. A difference of this magnitude is likely due to the fact that the seed crystals used in the growth of the hybrid membranes exceeded that of those used in the growth of pure ZIF-8 membranes. Our SEM results pertaining to morphology indicate that the quality of pure ZIF-8 membranes is on par with that of the ZIF-L@ZIF-8 hybrids, in terms of homogeneity and the absence of defects.

Computational and simulated XRD were applied to investigate the crystal structure and orientation of the ZIF-L seed layer and ZIF-L@ZIF-8 hybrid membrane (Fig. 3). GIXRD patterns (Fig. 3b) of the ZIF-L seed layer were compared with powder XRD patterns using the crystallographic information file (*.CIF file) of ZIF-L (Fig. 3a). The low signal-to-noise ratio shown in the GIXRD patterns of the ZIF-L seed layer is probably due to the discrete formation of seed crystals. Fig. 3d presents GIXRD patterns of ZIF-L@ZIF-8 hybrid membranes, showing peaks from ZIF-L (Fig. 3a) as well as ZIF-8 (Fig. 3c) crystals. This provides unambiguous evidence that the hybrid membrane comprises ZIF-L as well as ZIF-8. The {200} reflection of ZIF-8 in the experimentally-derived GIXRD patterns of the ZIF-L@ZIF-8 hybrid membrane is more pronounced than in simulated powder XRD patterns. This suggests that the preferred <100> orientation of the ZIF-8 crystals in the hybrid membranes can be attributed to the growth of ZIF-8 crystals on its pseudopolymorph, ZIF-L. The preferred orientation of the ZIF-8 crystals is likely due to the large area of facets in the [001] direction of the ZIF-L seed crystals, which may have favored the heteroepitaxial growth of ZIF-8 on ZIF-L. Several methods have been devised to control the crystal orientation of ZIF-8 membranes.[29, 33, 51] XRD patterns with a wider 2θ-range and the FT-IR spectra of the ZIF-L seed layer and ZIF-L@ZIF-8 hybrid membranes are presented in ESI,† Fig. S3 and S4. In the FT-IR spectra, peaks from ZIF-8 as well as ZIF-L were observed in the ZIF-L@ZIF-8 hybrid membranes, which provides additional supporting evidence for the success of hybrid formation.

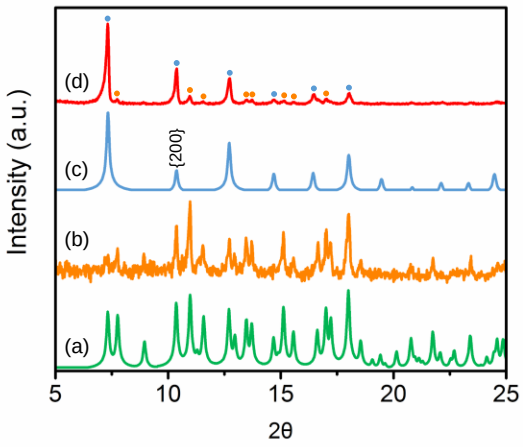

Fig. 3. Simulated powder XRD patterns: (a) ZIF-L and (c) ZIF-8. Experimentally-derived GIXRD patterns: (b) ZIF-L seed layer and (d) ZIF-L@ZIF-8 membrane. The blue dots in (d) indicate reflections from ZIF-8 and the orange dots in (d) indicate reflections from ZIF-L.

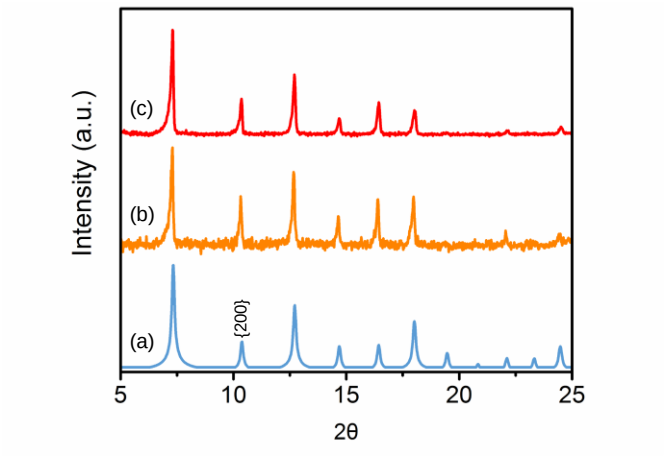

Fig. 4. Simulated powder XRD patterns of (a) ZIF-8; experimentally-derived GIXRD patterns of (b) ZIF-8 seed layer and (c) ZIF-8 membrane

Fig. 4 presents XRD patterns of ZIF-8 seed layer and pure ZIF-8 membrane obtained in simulations as well as experiments. Patterns in the GIXRD of ZIF-8 seed layer and pure ZIF-8 membrane and the simulated powder XRD of ZIF-8 are nearly identical. The experimental GIXRD pattern of ZIF-8 seed layer had a low signal-to-noise ratio because ZIF-8 formed discrete crystals in that sample. The fact that the GIXRD patterns obtained in experiments are nearly identical to the powder XRD patterns obtained in simulations indicates that the preferred crystal orientation is absent from the ZIF-8 seed layer as well as the pure ZIF-8 membrane. This differs from our observation of the preferred crystal orientation in ZIF-L@ZIF-8 hybrids. The only difference between the synthesis of pure ZIF-8 and ZIF-L@ZIF-8 hybrid membranes was the seed crystal. Thus, it is possible that the use of high aspect ratio ZIF-L crystals is the primary reason for the control of crystal orientation in the membranes. XRD patterns of ZIF-8 seed layer and pure ZIF-8 membranes with a wider 2θ-range are presented in ESI,† Fig. S5.

Single Gas Permeation

The performance of pure ZIF-8 and ZIF-L@ZIF-8 hybrid membranes with regard to single gas permeation was evaluated using hydrogen, methane, nitrogen, and carbon dioxide, the results of which are summarized in Fig. 5a. In the case of pure ZIF-8 membranes, gas permeability decreased with an increase in the kinetic diameter of the permeate molecules. The permeability of ZIF-8 membranes obtained in this work is in good agreement with the results reported from ZIF-8 membranes prepared by various other methods.[13, 21] For all four of the probing molecules, ZIF-L@ZIF-8 membranes presented permeability values exceeding those of pure ZIF-8 membranes. Fig. 5b summarizes the ideal permeative selectivity (defined by the permeability ratio for two gas species) of the two types of membrane for various gas pairs. The selectivity of pure ZIF-8 membranes is closed to previously reported values for ZIF-8 membranes synthesized in aqueous phase.[23, 27, 52] The ZIF-L@ZIF-8 hybrid membrane is superior to pure ZIF-8 membranes with regard to the selectivity for hydrogen when dealing with the following gas pairs: H_2/CO_2, H_2/CH_4, and H_2/N_2. This makes the

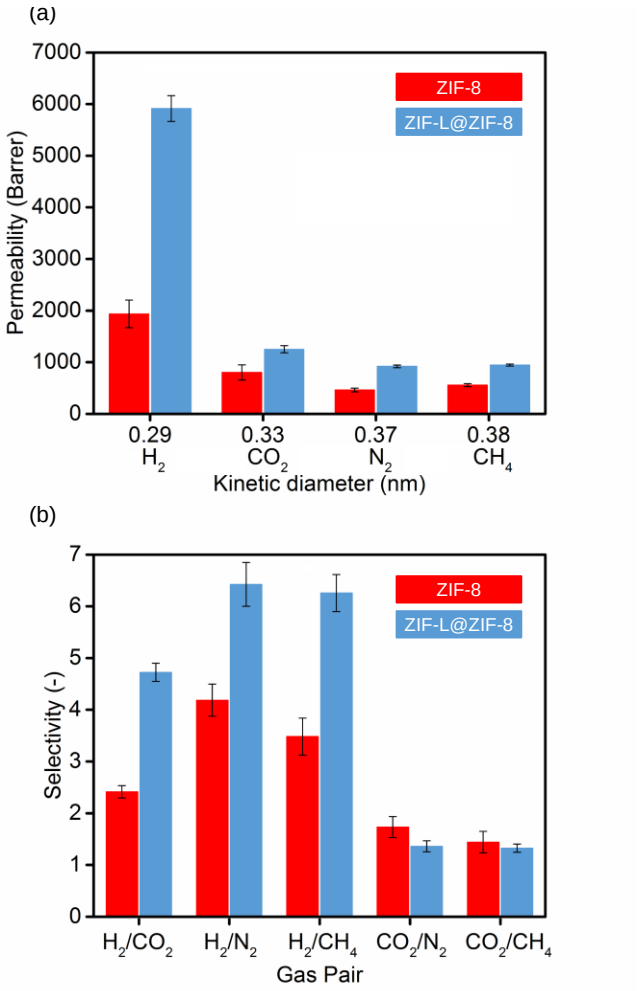

Fig. 5. (a) Single gas permeability of ZIF-8 and ZIF-L@ZIF-8 membranes; (b) ideal selectivity of ZIF-8 and ZIF-L@ZIF-8 membranes. 1 Barrer = 3.348 × 10−16 mol-m / (m²- s-Pa)

ZIF-L@ZIF-8 hybrid a better candidate for the purification of hydrogen. The excellent hydrogen selectivity of the hybrid membranes can be attributed to the fact that the incorporation of ZIF-L may result in an unusually high degree of hydrogen diffusivity. ZIF-L@ZIF-8 hybrid membranes possess CO_2 selectivity similar to that of pure ZIF-8 membranes for the gas pairs CO_2/N_2 and CO_2/CH_4. This is due to the fact that the permeability enhancement factors resulting from the incorporation of ZIF-L are nearly identical: CO_2 (1.56), N_2 (1.99), and CH_4 (1.70). The selectivity of ZIF-L@ZIF-8 hybrids is nearly the same as that of ZIF-8; however, the performance of these membranes is still considered to be higher than that of pure ZIF-8 due to higher permeability for CO_2. The single gas permeation under various feed pressure was also performed and summarized in ESI,† Fig. S6. The separation performance of the ZIF-L@ZIF-8 membranes stayed constant under different feed pressure, suggesting these membranes have minimal amount of defect spots.[53]

The fact that ZIF-L@ZIF-8 hybrid possesses permeability superior to that of pure ZIF-8 can be attributed to two distinct characteristics of the ZIF-L@ZIF-8 hybrid membranes: the preferred orientation of ZIF-8 crystals in the ZIF-L@ZIF-8, or

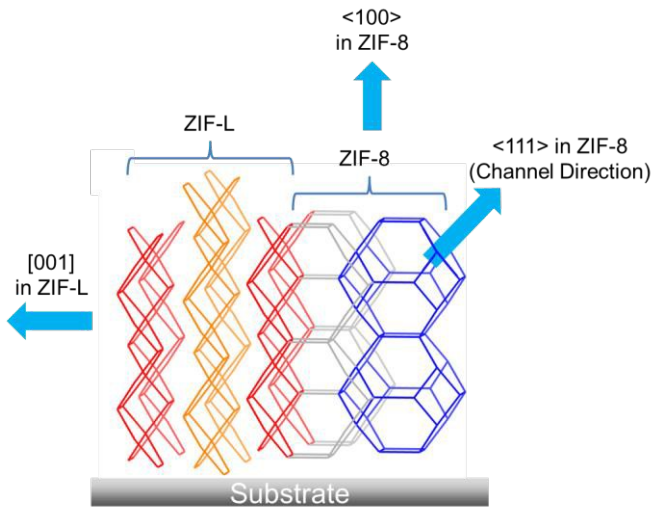

Fig. 6. Proposed microstructure of ZIF-L@ZIF-8 hybrid membrane

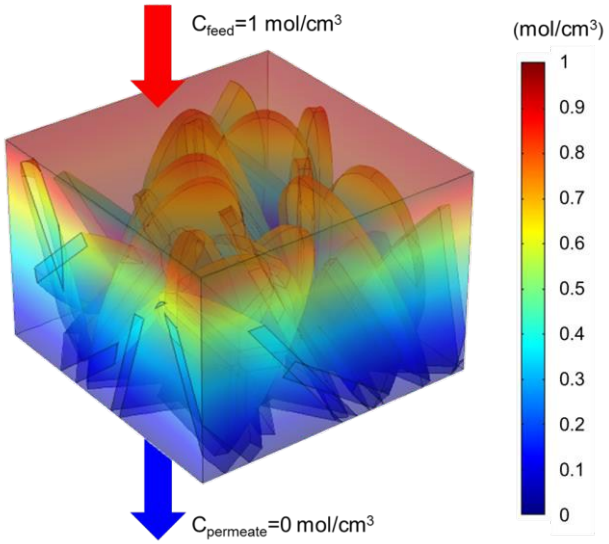

Fig. 7. Representative concentration profile (simulated) of ZIF-L@ZIF-8 hybrid membrane

the incorporation of ZIF-L within the hybrid membranes. ZIF-8 crystals oriented in the <100> direction are unlikely to enhance the permeation because the main channels for the molecular diffusion in ZIF-8 are in the <111> direction (Fig. 6). We therefore deduce that the incorporation of ZIF-L in the hybrid membrane (the intrinsic diffusivity of which may exceed that of ZIF-8),[42, 54] is more likely to account for the high degree of molecular permeability. The incorporation of ZIF-L into the membranes had a greater effect on hydrogen permeability than on the other three gas species tested in this study, which implies that ZIF-L has abnormally high hydrogen diffusivity. In the following section we discuss the simulation of mass transfer through consideration of the quantitative experiment results of permeation.

Simulation of Mass Transfer in Membranes at the Microscopic Level

We performed simulations of mass transfer in these hybrid membranes at the microscopic level to elucidate the effects of incorporating ZIF-L into ZIF-8 membranes on separation performance. Mass transfer was modeled on Fick's law of diffusion (Eq 1.). The methodology we used for the simulation of mass transfer in heterogeneous membranes is detailed in our previous work.[45-47] In principle, providing a numerical solution to Fick's diffusion equation yields a concentration profile in the hybrid membrane (Fig. 7). The permeability of the (simulated) membrane was deduced from the concentration distribution and then compared with the permeability values obtained in experiments. In the simulations, the dimensions of ZIF-L nanoflakes resembled their realistic dimensions. In particular, the long axis, short axis, and the thickness were 5, 2, and 0.2 μm, respectively. Two material properties (diffusivity and solubility), must be determined for the performance of simulations. The CO_2 and CH_4 solubility values of ZIF-8[48] and ZIF-L[41] were obtained from the literature. It was assumed that the H_2 and N_2 solubility values of ZIF-8 were identical. The diffusivity of ZIF-8 was derived from our measured results for the permeability of pure ZIF-8 membranes (since permeability is a product of diffusivity and solubility). The diffusivity of ZIF-L was adjusted until the simulated permeability of ZIF-L@ZIF-8 hybrids matched the values obtained in experiments. Fig. 8 presents a comparison of simulation and experiment results pertaining to the diffusivity of ZIF-L@ZIF-8 hybrid membranes. Among the four gas species tested in this study (H_2, CH_4, N_2, and CO_2), our simulation results were in excellent agreement with the experiment data, thereby demonstrating the validity of the proposed methodology for the modeling of mass transfer in the hybrid ZIF membranes at the microscopic level. The solubility values of ZIF-8 and ZIF-L are summarized in Fig. 9a, and the derived diffusivity of ZIF-L for various gaseous species is presented in Fig. 9b. The gaseous solubility of ZIF-8 and ZIF-L are similar for all of the gaseous species discussed in this work except for CO_2, for which ZIF-L

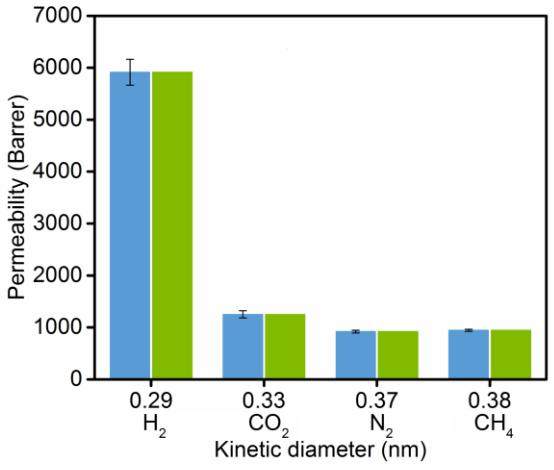

Fig. 8. Experimentally-derived and simulated permeability values of ZIF-L@ZIF-8 membrane.

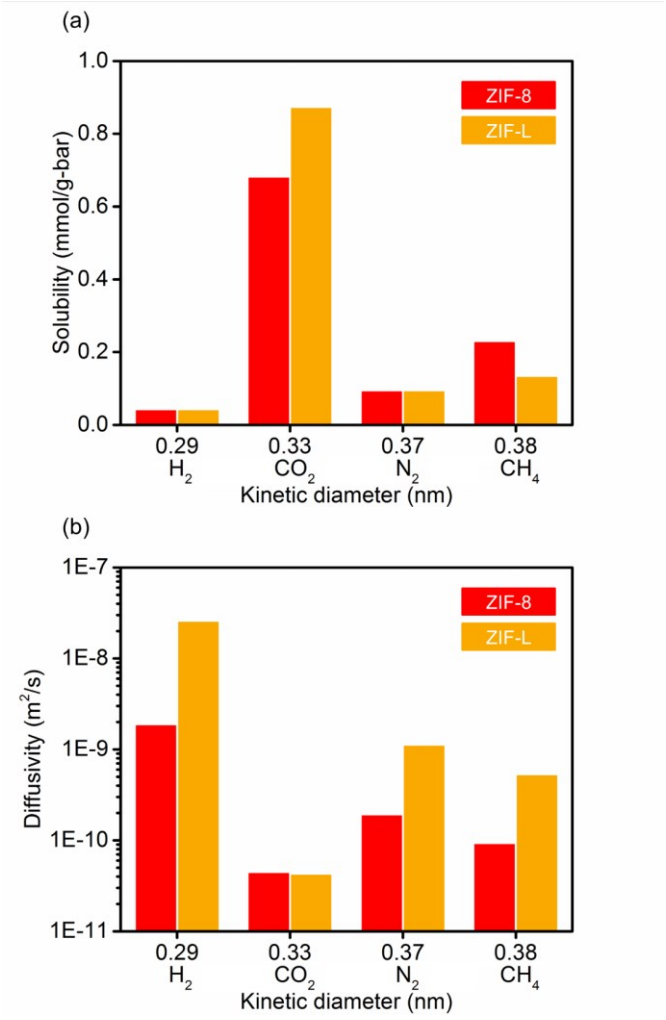

Fig. 9. (a) Solubility values of ZIF-8 and ZIF-L used for the simulations of mass transfer; (b) diffusivity of ZIF-8 used for the simulation of mass transfer and diffusivity of ZIF-L obtained from the same simulations

presents higher solubility. In contrast, the diffusivity of ZIF-L for H_2, N_2, and CH_4 is significantly higher than that of ZIF-8. In particular, the diffusivity of ZIF-L for H_2 is an order of magnitude higher than that of ZIF-8. The diffusivity and solubility of ZIF-8 and ZIF-L explain our experimental finding in which the ZIF-L@ZIF-8 hybrid membrane outperformed pure ZIF-8 membranes in terms of permeability and selectivity for hydrogen. The higher diffusivity of ZIF-L may be due to its layered crystal structure in which the ZIF-L crystal is formed through the two-dimensional assembly of layers in the *c*-direction with hydrogen bonds (non-covalent bonds). Interlayer spacing of 3.97 Å allows for high-throughput molecular diffusion. As shown in Fig. 6, the orientation of ZIF-L crystals in the ZIF-L@ZIF-8 hybrid membrane enable the transfer of mass through their interlayer spacing, which results in high permeability.

Conclusions

In this study, we introduce the concept of pseudopolymorphic seeding for the rational synthesis of hybrid membranes with zeolitic imidazolate frameworks (ZIFs). The efficacy of this approach was demonstrated using ZIF-L as seed crystals for the growth of its pseudopolymorphic crystal ZIF-8 within dense membranes. The key benefits of this rational approach to the synthesis of hybrid ZIF membranes are two-fold. First, it enables the use of materials with superior processability (i.e. ZIF-8) to serve as the matrix phase, in conjunction with materials possessing superior separation performance (i.e. ZIF-L) to serve as the filler phase with the aim of enhancing the separation performance of the hybrid membranes. Second, the fact that the seed crystals and the grown crystals are pseudopolymorphs guarantees good interfacial affinity between the two crystals and helps to prevent the formation of defects within the membranes.

This paper reports the synthesis of ZIF-L@ZIF-8 hybrid membranes with a ZIF-L volume fraction of approximately 28%. ZIF-8 crystals grown on ZIF-L seed crystals exhibited a preferred <100> orientation. ZIF-L@ZIF-8 hybrid membranes present higher molecular permeability for H_2, N_2, CH_4, and CO_2 and higher hydrogen selectivity, compared to pure ZIF-8 membranes. Simulations of diffusion at the microscopic scale were performed to compare these two types of membranes with regard to mass transfer. The superior separation performance of ZIF-L@ZIF-8 hybrid membranes can be attributed to the intrinsically high diffusivity of ZIF-L for hydrogen. The method presented in this study for the design and synthesis of hybrid membranes via pseudopolymorphic seeding could be extended to other metal organic frameworks or crystalline microporous/mesoporous membranes.

Acknowledgements

This work was supported by the Ministry of Science and Technology (MOST) of Taiwan (MOST 104-2628-E-002-009-MY3 and MOST 105-2923-E-002-002-MY2) and National Taiwan University (NTU-CDP-104R781 and NTU-CDP-105R7814). We would like to thank Chin-Yan Lin and Ya-Yun Yang in the Electron Microscope Unit of Instrument Center at National Taiwan University for assistance in obtaining SEM images. We would also like to thank Professor Huanting Wang at Monash University for generously providing the CIF file of ZIF-L crystal.

Notes and references

1. F. Gallucci, E. Fernandez, P. Corengia and M. V. Annaland, *Chem. Eng. Sci.*, 2013, **92**, 40.
2. P. Bernardo, E. Drioli and G. Golemme, *Ind. Eng. Chem. Res.*, 2009, **48**, 4638.
3. Y. Zhang, J. Sunarso, S. M. Liu and R. Wang, *Int. J. Greenhouse Gas Control*, 2013, **12**, 84.
4. N. Y. Du, H. B. Park, M. M. Dal-Cin and M. D. Guiver, *Energy Environ. Sci.*, 2012, **5**, 7306.
5. D. E. Sanders, Z. P. Smith, R. L. Guo, L. M. Robeson, J. E. McGrath, D. R. Paul and B. D. Freeman, *Polymer*, 2013, **54**, 4729.
6. L. M. Robeson, *J. Membr. Sci.*, 1991, **62**, 165.
7. Z. P. Lai, G. Bonilla, I. Diaz, J. G. Nery, K. Sujaoti, M. A. Amat, E. Kokkoli, O. Terasaki, R. W. Thompson, M. Tsapatsis and D.

G. Vlachos, *Science*, 2003, **300**, 456.
8. S. J. Yang, M. Lach-hab, Vaisman, II, E. Blaisten-Barojas, X. A. Li and V. L. Karen, *J. Phys. Chem. Ref. Data*, 2010, **39**, 45.
9. M. W. Deem, R. Pophale, P. A. Cheeseman and D. J. Earl, *J. Phys. Chem. C*, 2009, **113**, 21353.
10. A. Phan, C. J. Doonan, F. J. Uribe-Romo, C. B. Knobler, M. O'Keeffe and O. M. Yaghi, *Acc. Chem. Res.*, 2010, **43**, 58.
11. D. W. Lewis, A. R. Ruiz-Salvador, A. Gomez, L. M. Rodriguez-Albelo, F. X. Coudert, B. Slater, A. K. Cheetham and C. Mellot-Draznieks, *CrystEngComm*, 2009, **11**, 2272.
12. Y. Q. Tian, C. X. Cai, Y. Ji, X. Z. You, S. M. Peng and G. H. Lee, *Angew. Chem., Int. Ed.*, 2002, **41**, 1384.
13. B. R. Pimentel, A. Parulkar, E. K. Zhou, N. A. Brunelli and R. P. Lively, *ChemSusChem*, 2014, **7**, 3202.
14. K. S. Park, Z. Ni, A. P. Cote, J. Y. Choi, R. D. Huang, F. J. Uribe-Romo, H. K. Chae, M. O'Keeffe and O. M. Yaghi, *Proc. Natl. Acad. Sci. U. S. A.*, 2006, **103**, 10186.
15. R. Banerjee, A. Phan, B. Wang, C. Knobler, H. Furukawa, M. O'Keeffe and O. M. Yaghi, *Science*, 2008, **319**, 939.
16. K. Sumida, D. L. Rogow, J. A. Mason, T. M. McDonald, E. D. Bloch, Z. R. Herm, T. H. Bae and J. R. Long, *Chem. Rev.*, 2012, **112**, 724.
17. D. Farrusseng, S. Aguado and C. Pinel, *Angew. Chem., Int. Ed.*, 2009, **48**, 7502.
18. L. E. Kreno, K. Leong, O. K. Farha, M. Allendorf, R. P. Van Duyne and J. T. Hupp, *Chem. Rev.*, 2012, **112**, 1105.
19. P. Horcajada, R. Gref, T. Baati, P. K. Allan, G. Maurin, P. Couvreur, G. Ferey, R. E. Morris and C. Serre, *Chem. Rev.*, 2012, **112**, 1232.
20. M. Shah, M. C. McCarthy, S. Sachdeva, A. K. Lee and H. K. Jeong, *Ind. Eng. Chem. Res.*, 2012, **51**, 2179.
21. J. Yao and H. Wang, *Chem. Soc. Rev.*, 2014, **43**, 4470.
22. H. Bux, F. Liang, Y. Li, J. Cravillon, M. Wiebcke and J. Caro, *J. Am. Chem. Soc.*, 2009, **131**, 16000.
23. Y. Pan, B. Wang and Z. Lai, *J. Membr. Sci.*, 2012, **421**, 292.
24. M. C. McCarthy, V. Varela-Guerrero, G. V. Barnett and H.-K. Jeong, *Langmuir*, 2010, **26**, 14636.
25. S. R. Venna and M. A. Carreon, *J. Am. Chem. Soc.*, 2010, **132**, 76.
26. Y. Pan, T. Li, G. Lestari and Z. Lai, *J. Membr. Sci.*, 2012, **390**, 93.
27. K. Huang, Z. Dong, Q. Li and W. Jin, *Chem. Commun.*, 2013, **49**, 10326.
28. Y. Zhu, Q. Liu, J. Caro and A. Huang, *Sep. Purif. Technol.*, 2015, **146**, 68.
29. K. Kida, K. Fujita, T. Shimada, S. Tanaka and Y. Miyake, *Dalton Trans.*, 2013, **42**, 11128.
30. S. Tanaka, T. Shimada, K. Fujita, Y. Miyake, K. Kida, K. Yogo, J. M. Denayer, M. Sugita and T. Takewaki, *J. Membr. Sci.*, 2014, **472**, 29.
31. X. Zhang, Y. Liu, L. Kong, H. Liu, J. Qiu, W. Han, L.-T. Weng, K. L. Yeung and W. Zhu, *J. Mater. Chem. A*, 2013, **1**, 10635.
32. Y. Hu, X. Dong, J. Nan, W. Jin, X. Ren, N. Xu and Y. M. Lee, *Chem. Commun.*, 2011, **47**, 737.
33. H. Bux, A. Feldhoff, J. Cravillon, M. Wiebcke, Y.-S. Li and J. Caro, *Chem. Mater.*, 2011, **23**, 2262.
34. Y. Liu, N. Wang, J. H. Pan, F. Steinbach and J. Caro, *J. Am. Chem. Soc.*, 2014, **136**, 14353.
35. H. T. Kwon, H. K. Jeong, A. S. Lee, H. S. An and J. S. Lee, *J. Am. Chem. Soc.*, 2015, **137**, 12304.
36. H. T. Kwon and H.-K. Jeong, *J. Am. Chem. Soc.*, 2013, **135**, 10763.
37. J. Yao, D. Dong, D. Li, L. He, G. Xu and H. Wang, *Chem. Commun.*, 2011, **47**, 2559.
38. A. J. Brown, N. A. Brunelli, K. Eum, F. Rashidi, J. R. Johnson, W. J. Koros, C. W. Jones and S. Nair, *Science*, 2014, **345**, 72.
39. S. J. Noh, S. P. Yoon, J. Han, S. Park and J. Kim, *J. Nanosci. Nanotechnol.*, 2015, **15**, 575.
40. E. Shamsaei, Z. X. Low, X. C. Lin, A. Mayahi, H. Y. Liu, X. W. Zhang, J. Z. Liu and H. T. Wang, *Chem. Commun.*, 2015, **51**, 11474.
41. R. Chen, J. Yao, Q. Gu, S. Smeets, C. Baerlocher, H. Gu, D. Zhu, W. Morris, O. M. Yaghi and H. Wang, *Chem. Commun.*, 2013, **49**, 9500.
42. Z. X. Zhong, J. F. Yao, R. Z. Chen, Z. Low, M. He, J. Z. Liu and H. T. Wang, *J. Mater. Chem. A*, 2015, **3**, 15715.
43. W. C. Lee, H. T. Chien, Y. Lo, H. C. Chiu, T. P. Wang and D. Y. Kang, *ACS Appl. Mater. Interfaces*, 2015, **7**, 18353.
44. Z.-X. Low, J. Yao, Q. Liu, M. He, Z. Wang, A. K. Suresh, J. Bellare and H. Wang, *Cryst. Growth Des.*, 2014, **14**, 6589.
45. T. Singh, D. Y. Kang and S. Nair, *J. Membr. Sci.*, 2013, **448**, 160.
46. T. P. Wang and D. Y. Kang, *J. Membr. Sci.*, 2015, **485**, 123.
47. A.-C. Yang, C.-H. Liu and D.-Y. Kang, *J. Membr. Sci.*, 2015, **495**, 269.
48. C. Zhang, R. P. Lively, K. Zhang, J. R. Johnson, O. Karvan and W. J. Koros, *J. Phys. Chem. Lett.*, 2012, **3**, 2130.
49. Y. Liu, N. Wang, L. Diestel, F. Steinbach and J. Caro, *Chem. Commun.*, 2014, **50**, 4225.
50. D. F. Liu, X. L. Ma, H. X. Xi and Y. S. Lin, *J. Membr. Sci.*, 2014, **451**, 85.
51. C. Hou, Q. Xu, J. Peng, Z. Ji and X. Hu, *ChemPhysChem*, 2013, **14**, 140.
52. Y. Pan and Z. Lai, *Chem. Commun.*, 2011, **47**, 10275.
53. M. A. Yu, H. H. Funke, R. D. Noble and J. L. Falconer, *J. Am. Chem. Soc.*, 2011, **133**, 1748.
54. Z.-X. Low, A. Razmjou, K. Wang, S. Gray, M. Duke and H. Wang, *J. Membr. Sci.*, 2014, **460**, 9.